Proceedings of the International Gas Turbine Congress 2003 Tokyo
November 2-7, 2003

**IGTC2003Tokyo OS-107**

# Prototyping of Small-sized Two-dimensional Radial Turbines

Kazuo MATSUURA[1], Chisachi KATO[2], Haruo YOSHIKI[3], Eito MATSUO[4],
Hiroyuki IKEDA[5], Katsuhiko NISHIMURA[6] and Rajesh SAPKOTA[1]

[1] Graduate Student, [2] Professor
[3] Professor Emeritus, [4] Collaborative Researcher
[5] Former Graduate Student, [6] Research Associate
Institute of Industrial Science, The University of Tokyo
4-6-1 Komaba, Meguro-ku, Tokyo 153-8505, JAPAN
Phone: +81-3-5452-6098 ext. 57414, E-mail: kazuo@iis.u-tokyo.ac.jp

**ABSTRACT**

Small-sized 2D and 3D radial turbines are designed, fabricated and their aerodynamic performance is experimentally measured. Also, with numerical simulation, major loss-generating factors are investigated.

Adiabatic efficiencies of the developed 2D radial turbines are very low when compared to those of the developed 3D turbines. The reduction of efficiency can be mainly attributed to exducers, nozzle wake regions and rotor blades' surfaces.

Using Computational Fluid Dynamics (CFD) results, loss characteristics of 2D turbines and design philosophy required for developing efficient 2D turbines are discussed.

## INTRODUCTION

Ultra-micro-scale radial gas turbines with outputs less than several kW are expected for practical uses in various fields such as power sources for self-running robots, note PCs, portable telephones, or thrust generators for unmanned air vehicles (Yoshiki, 2001). In order to make ultra-micro-scale radial gas turbines practicable, we have to solve various problems such as realization of stable combustion in microscopic regions, development of highly efficient turbines, compressors and high-speed air bearings, improvement in cycle efficiencies by implementing recuperators, and development of high rotational speed generators (Epstein, et al., 1997). In particular, improvement in adiabatic efficiencies of radial turbines which generate shaft outputs or thrusts is one of the crucial problems on which realization of such a cycle depends (Epstein, et al., 2000).

It is difficult to fabricate ultra-micro-scale radial gas turbines with impeller tip radii less than several millimeters by conventional mechanical manufacturing, and Micro Electro Mechanical Systems (MEMS) processings such as Chemical Vapor Deposition (CVD) are expected to become the major fabrication process of such a device. In case where nozzles and impellers are manufactured with MEMS processings, their shapes must be 2D due to the manufacturing constraints. For 3D radial turbines, design methods have been almost established (Isomura, et al., 2001) and there are various data requisite for designing them (Matsuo, 1998, Tanaka, et al., 2002). For 2D turbines, however, there are few reports, and design methods or philosophies have not been established yet. Therefore, in this research, 2D radial turbines are designed, fabricated and their aerodynamic performance is experimentally measured. Also, with numerical simulations based on CFD, major loss-generating factors are investigated. In this paper, some important results obtained from experiments and numerical simulations are presented.


Manuscript Received on May 21, 2003

**Table. 1 Design Specifications of 2D turbines**

| | Type A | Type B | Type C |
|---|---|---|---|
| Pressure Ratio | ← | 2.91 | → |
| Turbine Inlet Temperature [K] | ← | 1223 | → |
| Rotational Speed [rpm] | $2.4\times10^5$ | $2.4\times10^5$ | $1.89\times10^5$ |
| Mass Flow Rate [kg/s] | 0.030 | 0.030 | 0.019 |
| Impeller Outer Diameter [mm] | ← | 40 | → |
| Nozzle Outer Diameter [mm] | ← | 52 | → |
| Number of Blades | 15 | 15 | 16 |
| Number of Vanes | ← | 17 | → |
| Blade (Vane) Height [mm] | 4.8 | 3.6 | 3.2 |

## AERODYNAMIC DESIGN

In the present research, 2D and 3D radial turbines are designed, fabricated and experimented (Ikeda, 2003). Regarding the design of 2D turbines, 3 types viz. Type A, B and C are manufactured (Table. 1). Type A is a turbine designed for attaining high adiabatic efficiency; Type B is designed for attaining large mass flow rate with a relatively low blade height. Compared to 3D turbine, design conditions from structural aspects are stringent at the same impeller diameters and rotational speeds. In this regard, Type C is designed for attaining high efficiency with lower rotational speed. Regarding the 3D turbines, two types of turbines with mass flow rate of 30 g/s and 50 g/s are manufactured for comparison with 2D turbines.

All the 2D turbines have an impeller outer diameter of 40 mm. At its design point, each turbine is expected to possess the following performance. Type A and Type B turbines are designed to have 30 g/s mass flow rates and generate approximately 7 kW at a pressure ratio of 2.91, rotational speed of $2.4\times10^5$ rpm and turbine

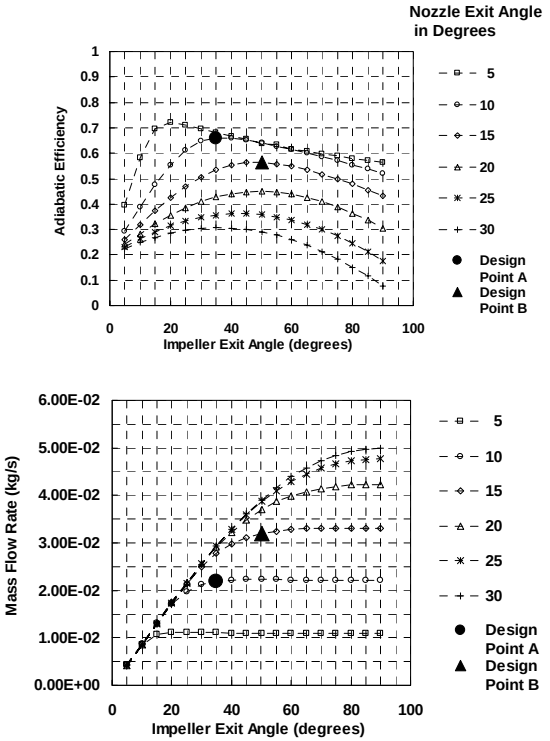


**Fig. 1 Predicted adiabatic efficiencies and mass-flow rates for Type A and Type B turbines.**

inlet temperature of 1223 K. Type C turbine is designed to have 19 g/s mass flow rate and generate approximately 4 kW at a rotational speed of $1.89 \times 10^5$ rpm.

Aerodynamic designs are based on velocity triangles evaluated at inlet and outlet positions of nozzles and turbine rotors. Considering the two dimensionalities and low Reynolds number effects, velocity coefficients of the nozzle and rotor are assumed to be 0.85 and 0.80, respectively (Mizumachi, 1958). The variations of the predicted adiabatic efficiencies and mass flow rates with respect to the impellers' exit angles are shown in Fig. 1. Nozzle exit angles are parameterized in these figures. Note that all the exit angles are measured from the tangential directions. In these predictions, turbine incidence loss and turbine tip leakage loss are included but exhaust loss at turbine exits is not.

By decreasing throat areas of nozzles, adiabatic efficiency of the turbine can be increased but at the same time, the mass flow decreases. In addition to that, flows may become unstable because of strong swirls immediately after the nozzles. From the above considerations, point A and B are chosen to be the design point for Type A and B turbines respectively. Type C turbine is designed with a similar method, which is not described here.

The degrees of reaction of the design points are 0.60, 0.74 and 0.74 for Type A, Type B and Type C. These values are rather high when compared to those of general 3D radial turbines, which is due to inherent flow expansion caused by relative decrease of cross sectional areas in 2D rotor passages.

Photographs and velocity triangles at the inlets and outlets of turbines manufactured in this research are shown in Figs. 2 through 5.

The material of rotors is AL2316 for aerodynamic test.

## AERODYNAMIC TEST

In general, it is difficult to evaluate aerodynamic performance of turbines precisely by hot gas tests. In the present research, that of the developed turbines is evaluated by cold flow tests.

Photographs and schematic views of the experimental apparatus are shown in Fig. 6. Pressurized air is supplied from the air source ① to drive the test turbine ② through the control valve CV2.

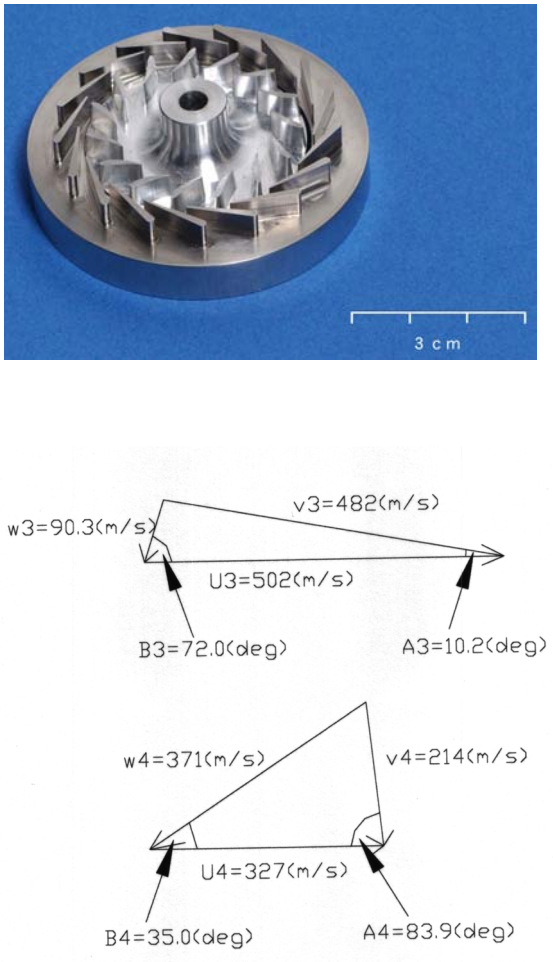


**Fig. 2 Fabricated Type A turbine (Degree of Reaction=0.60) (upper: Photograph, middle: Designed velocity triangles at impeller's inlet ant outlet, lower: Plane view of the rotor from the rotational axis direction)**

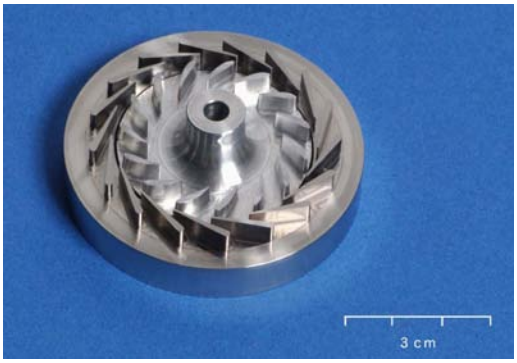


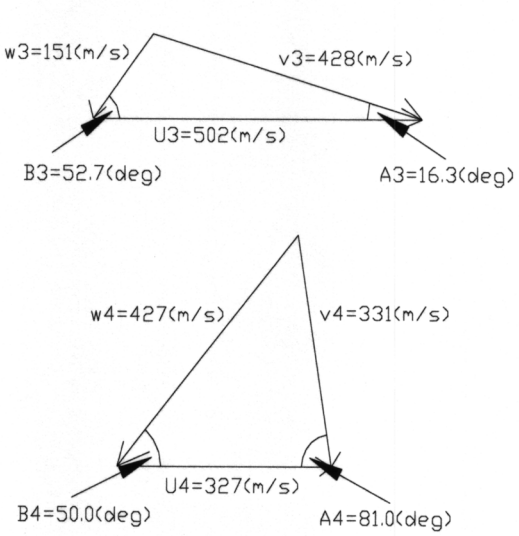


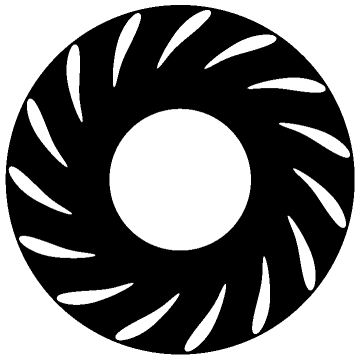

**Fig. 3 Fabricated Type B turbine (Degree of Reaction=0.74). (upper: Photograph, middle: Designed velocity triangles at impeller's inlet ant outlet, lower: Plane view of the rotor from the rotational axis direction)**


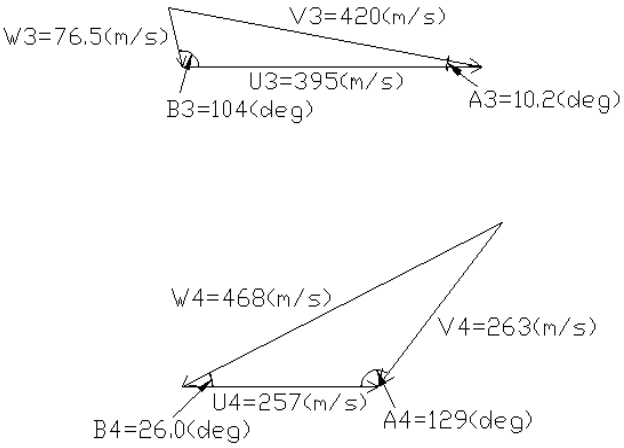


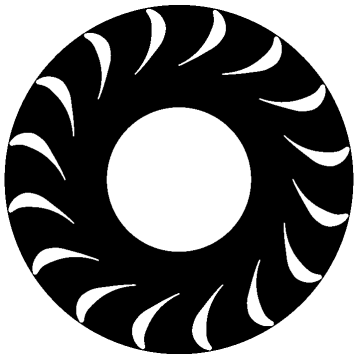

**Fig. 4 Fabricated Type C turbine (Degree of Reaction=0.74). (upper: Photograph, middle: Designed velocity triangles at impeller's inlet ant outlet, lower: Plane view of the rotor from the rotational axis direction)**

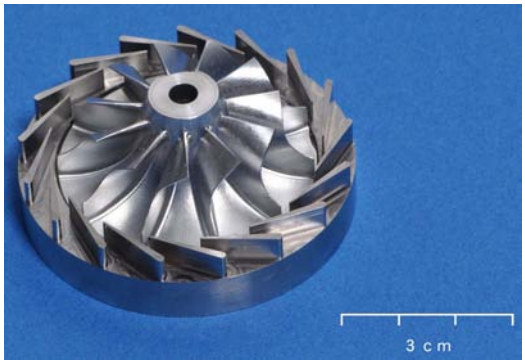


**Fig. 5 Fabricated 3D turbine (Degree of Reaction=0.48).**

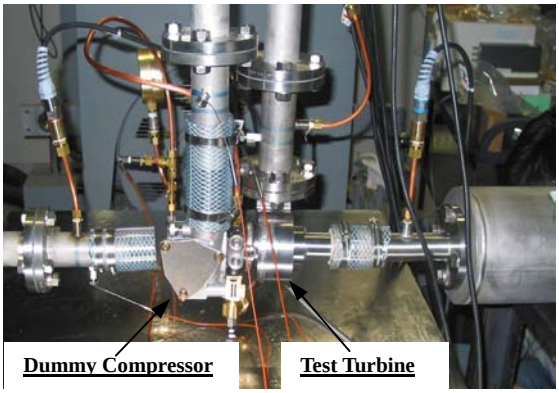


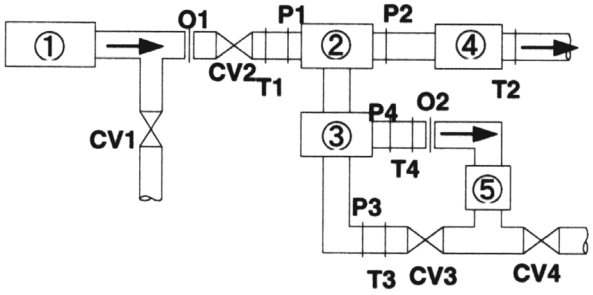


*①: Air Source, ②: Test Turbine, ③: Dummy Compressor, ④: Mixing Chamber, ⑤: Air Cooler, O1: Turbine Mass Flow Measuring Orifice, O2: Compressor Mass Flow Measuring Orifice, P1: Turbine Inlet Pressure, P2: Turbine Outlet Pressure, P3: Compressor Inlet Pressure, P4: Compressor Outlet Pressure, T1: Turbine Inlet Temperature, T2: Turbine Outlet Temperature, T3: Compressor Inlet Temperature, T4: Compressor Outlet Temperature, CV1 ~CV4: Control Valves*

**Fig. 6 Experimental set-up for aerodynamic-performance test.**

Outflows from the turbine are discharged to the atmosphere through the mixing chamber ④. The chamber is installed in order to homogenize the exhaust gas temperature while keeping the total temperature constant with heat insulating materials around it. On the other hand, the power generated by the turbine is absorbed by the dummy compressor ③ which is directly connected to the turbine with a single shaft. Outflows from the compressor ③ are cooled down in the air cooler ⑤, decompressed by the control valve CV3 etc. and restored to the inlet condition. By forming a closed compressor air loop, density of the working fluid and the mass flows can be adjusted in a wide range of compressor operating conditions.

In the present experiments, the rotational speed is taken as a variable parameter and set so that isentropic velocity ratio $U/C_0$ ranges from 0.3 to 0.8 at turbine pressure ratios of 1.5, 2.0 and 2.5, where U is the tip speed of the impeller and $C_0$ is the isentropic expansion velocity.

From measured rotational speeds, pressure ratios and temperatures, turbine adiabatic efficiencies are evaluated. In order to check the accuracy of the adiabatic efficiencies, sum of compressor absorption power and mechanical loss are evaluated and compared to turbine output. The absorption power is calculated from the compressor inlet, outlet temperatures (T3, T4) and mass flows (O2), and the loss is from mass flows of turbine lubrication oil and its temperature rise.

## EXPERIMENTAL RESULTS

Total–to-static adiabatic efficiencies of 2D turbines evaluated from the experimental results are shown in Fig. 7 with $U/C_0$ as the abscissa. Also shown in the same figure are the results of 3D turbines which are approximately of the same size as 2D counterparts and computational results of all types of turbines for comparison. At present, we have not completed all experiments. However, from experimental data of Type A and Type C turbines obtained so far, efficiency peaks are seem to lie around 65% at $U/C_0$ of 0.55. For Type B turbines, efficiency rises are seen to saturate near $U/C_0$ of 0.6, where the efficiency is about 55%. Compared to the measured efficiencies of the 3D turbines, these values are at least 15% lower.

With smaller scale turbines, further reductions in adiabatic efficiencies are expected due to low Reynolds number effects and tip leakage flows, etc.. Therefore, in order to make ultra-micro-scale radial gas turbines system practical, improvements in turbine adiabatic efficiencies are indispensable.

In the next section, possible reasons for the efficiency reductions of 2D turbine are investigated.

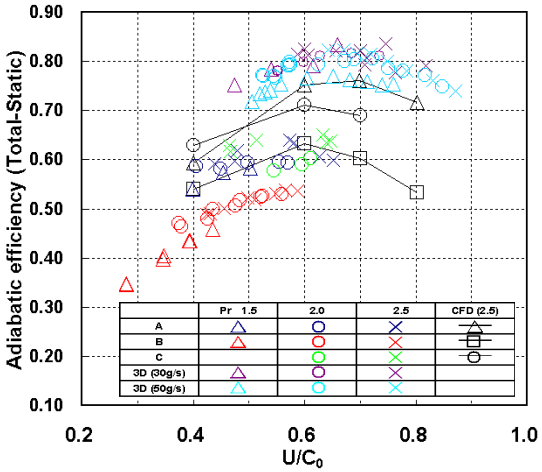


**Fig. 7 Measured and predicted total-to-static adiabatic efficiencies.**

## NUMERICAL SIMULATION OF INTERNAL FLOWS

In order to investigate major loss-generating factors in detail, steady numerical simulations based on 3D compressible Navier-Stokes equations with thin layer approximation were performed. The basic equations are described by absolute velocities seen from the stationary frame and rotational effects are treated by defining grid points' velocities and addition of Coriolis force terms. In these simulations, turbulence effects are treated by using Baldwin-Lomax turbulence model.

In ultra-micro-scale radial turbines, Reynolds numbers of internal flows range from a few thousands to several ten thousands and accurate predictions of transitional flows are considered to be important in estimating aerodynamic performance. However,

transition prediction is a difficult problem, and open to argument. In the present calculations, no special treatment for transition is made and the boundary layers are assumed to be all along turbulent. The computational grid used in the calculations for Type A turbine is shown in Fig. 8. Grids for other types of turbines are basically same. The calculation region is one pitch of blade passages for nozzle and rotor (rotor+exducer) and H-H topology grids are adopted for the present computations. Number of grid points for streamwise, pitchwise and spanwise directions are about 90, 35 and 35, respectively for both nozzle and rotor. Total number of grid points are approximately 220,000 points. Overlapping width between nozzle region and rotor region is 3 grid points, where physical values averaged in the pitchwise directions are interchanged. Effect of tip clearance is not modeled in the calculations. However, in these small diameter turbines, tip leakage loss is consider to become relatively large, and its influence on the turbine performance is estimated to a few percent decrease in adiabatic efficiency. Computations including the effects of tip clearance and transition are to be done in the future.

Concerning the boundary conditions, total temperature, total pressure and inflow angle are specified at the inlet boundary of a nozzle. At the rotor exit boundary, static pressure distributions equilibrated in radial direction are given. At wall boundary, adiabatic non-slip conditions are specified. Heat release from wall boundary is not considered in the present calculations.

With regard to the calculation conditions, velocity ratio $U/C_0$ is varied with the turbine pressure ratio and the nozzle inlet total temperature being fixed respectively to 2.5 and 50℃.

**Estimations of Entropy Generation**

In order to quantify loss-generating factors, the entire computational region is divided into 6 sub-regions and entropy generation in each of the sub-regions is estimated. The results are summarized in Fig. 9. Region 1 corresponds to inflow region in the nozzle calculation region, which ranges from the inflow boundary position to the leading edge of the nozzle vane. Region 2 corresponds to the nozzle passage region which ranges from the leading edge of the nozzle vane to the trailing edge of the nozzle vane. Region 3 corresponds to the outflow region which ranges from the trailing edge of the nozzle vane to the outflow boundary of the nozzle region. Similar to the division of the nozzle, the rotor calculation region is also divided into three sub-regions; Region 4 through Region 6, with taking position of the leading edge and the trailing edge into consideration.

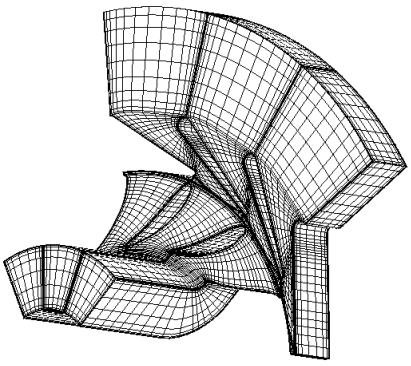

**Fig. 8 Computational grids for Type A turbine.**

**Nozzles**

Computed iso-Mach contours in the nozzle passages at the mid span are shown in Fig. 10. Although small separated regions are identified near the leading edges of the nozzles, flows expand smoothly in the passages without any noticeable evidence of loss generation. On the other hand, large wake regions exist downstream the trailing edge of the nozzles. As can be seen from

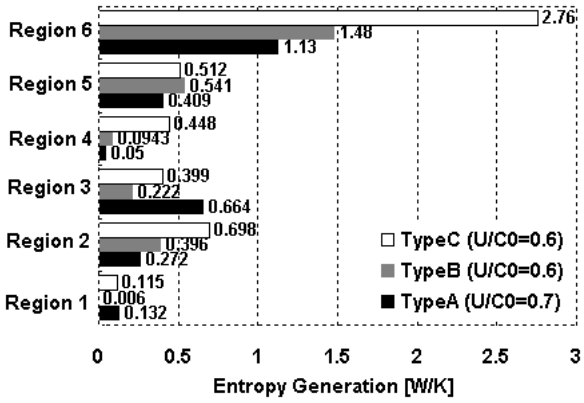


**Fig. 9 Entropy generation for 3 types of turbines**

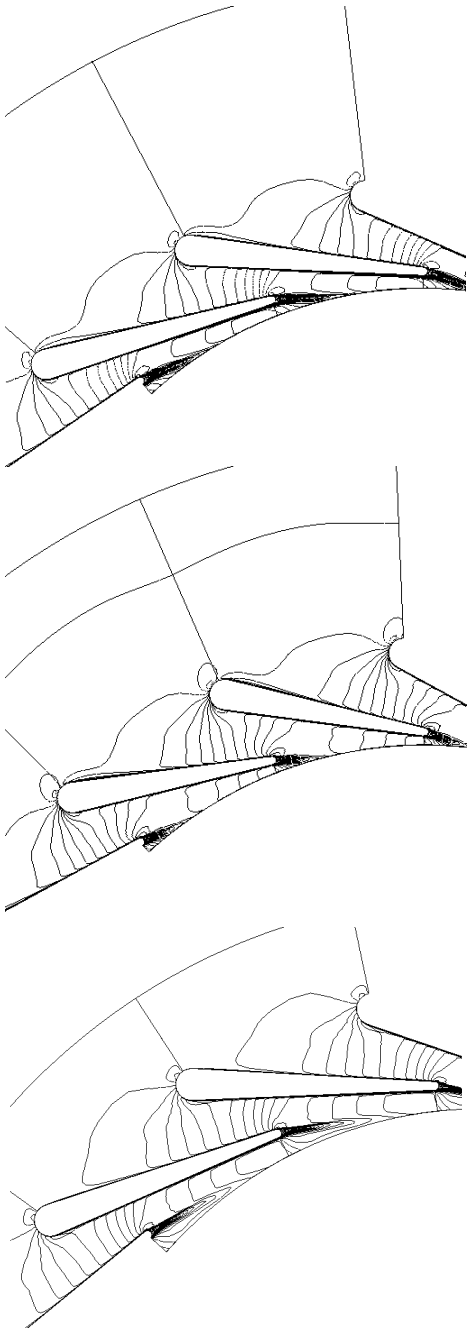

**Fig. 10 Computed iso-Mach contours in nozzle passages at midspan (upper: Type A turbine at $U/C_0$=0.7, middle: Type B turbine at $U/C_0$=0.6, lower: Type C turbine at $U/C_0$=0.6).**

Fig. 9, large loss occurs in that region. For the case of Type A turbine, the loss accounts to 25% of the overall loss. Kinetic energy of flow at the exit of nozzles is the highest in turbines, and large generation of loss can be one of the major causes for large reduction in adiabatic efficiencies.

In order to reduce loss near the trailing edges, it is necessary to make the trailing edge thickness thinner. But, the minimum thickness is limited by heat-resistant strength and process constraints, and therefore, further reductions in its thickness are considered to require improvements in materials and manufacturing processes.

**Turbine Rotors**

Computed iso-Mach contours in turbine rotors for Type A are shown Fig. 11. At inlets of rotor calculation regions, relative velocity vectors are also shown. As is described before, circumferencially averaged physical values are interchanged between nozzle and rotor regions. Therefore, nozzle wakes are simulated only in an averaged sense.

At the velocity ratio corresponding to the peak efficiency, incidence angle of the rotor inflow is nearly zero. Flow expands rather uniformly until the rotor blade's throat, but around 80% chord length, flows separate on the suction side as can also be confirmed from the static pressure distribution along the blade (Fig. 12). This separation decreases the blade work and is estimated to generate about 15% of the overall loss from generated entropy at Region 5 in Fig. 9. In Type A turbine rotor, the blade camberline is designed to make the flow turn downstream the throat. But, downstream the throats there are no longer cascade effects, and the flow does not expand further. Therefore, flow is most likely to separate from the blade surface. Turbine rotor exit flow is also considered to be greatly influenced by the pressure distribution at the succeeding exducer inlet. On the viewpoint of reducing loss near the rotor trailing edge, reconsiderations of both blade shapes and meridian shapes of exducers are nessesary.

Computed iso-Mach contours in turbine rotors for Type B are shown Fig. 13. The incidence angle of the rotor inflow is positive at velocity ratio of 0.6. As can be clearly seen from the surface pressure distribution (Fig. 12) and iso-Mach contours, boundary layer on the rotor suction side separates almost all chord. Since Type B turbine is designed to have a relatively large throat area, expansion of flow in the nozzle becomes insufficient compared to the rotor inlet tip speed. As the result of that, relative inflow angle to the rotors becomes small. Furthermore, turning angle of the relative flow in rotor passages become very small. As the result, with considering the blades are negative-cambered, boundary layers on the suction sides separate almost all the chord.

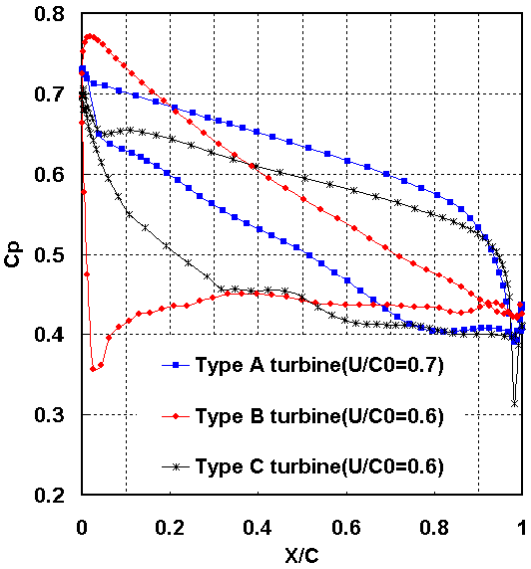


**Fig. 12 Distribution of static pressure along blade surface.**

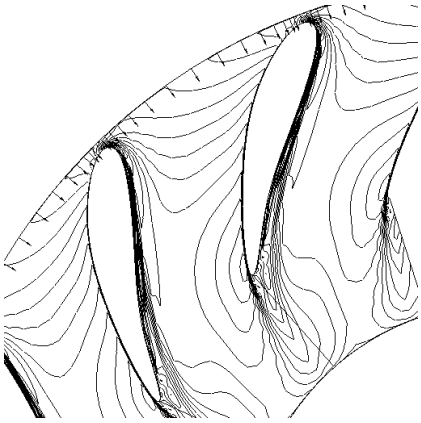

**Fig. 13 Computed iso-Mach contours in rotor passages at mid span (Type B turbine at $U/C_0$=0.6)**

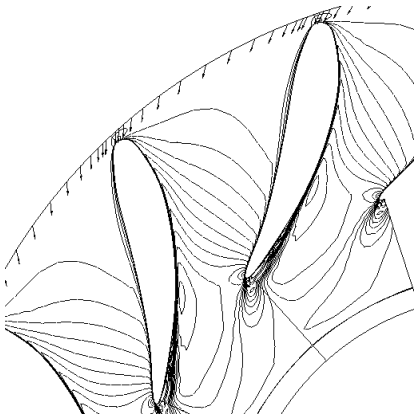

**Fig. 11 Computed iso-Mach contours in rotor passages at mid span (Type A turbine at $U/C_0$=0.7)**

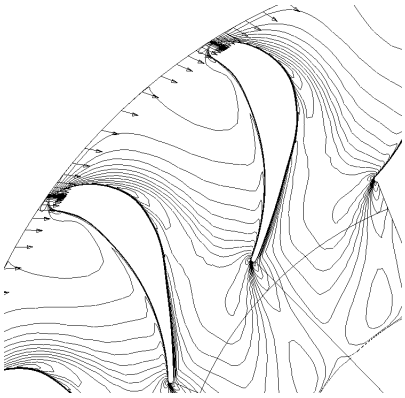

**Fig. 14 Computed iso-Mach contours in rotor passages at mid span (Type C turbine at $U/C_0$=0.6).**

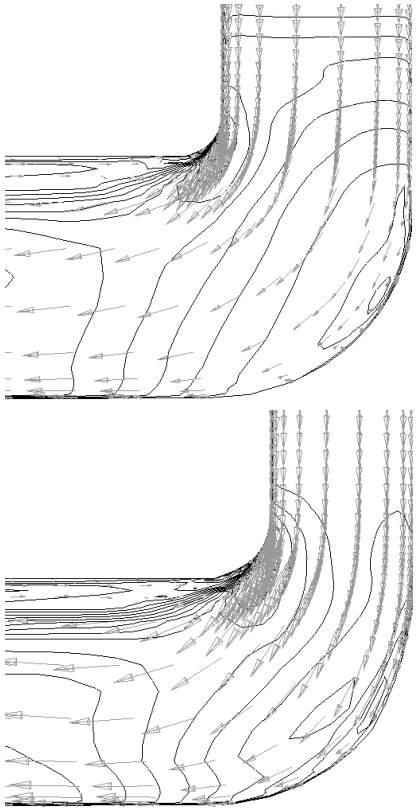

**Fig. 15 Computed iso-Mach contours in exducer (upper: Type A turbine at $U/C_0$=0.7, lower: Type B turbine at $U/C_0$=0.6).**

Computed iso-Mach contours in turbine rotor for Type C is shown in Fig. 14. As is described before, in order to realize ultra-micro-scale radial turbines, structure strength against high rotational speed is one of the crucial problems. Type C turbine rotor is designed to have efficiency peaks at a relatively low rotational speed compared to Type A and Type B turbines. Incidence angle of rotor inflow is nearly zero at velocity ratio 0.6. Flows expand rather suddenly in the first 30% chord on the suction side and uniformly on nearly all the pressure side, which are confirmed by the accumulation of iso-Mach number contours and also by the static pressure distribution along the blade (Fig. 12). Turning angle of the blade camberline is 77° , which is about twice that of Type A. Flow separation occurs at near 82% chord due to such a severe blade's curvature. This separation causes increasing the angle of relative rotor outflow and the absolute swirling velocity. As the result, adiabatic efficiency decreases.

Finally, computed iso-Mach contours in the exducer are presented in Fig. 15. Flow experiences abrupt turnings from radial direction to axial direction near the rotor exits. In all types of turbines, large separation occurs near the inlet of exducer.

In 2D turbines, because of large radius ratio of the leading edge to the trailing edge, radial components of absolute rotor exit velocities become inevitably large. These values are approximately 90m/s for the Type A turbine, 130m/s for both Type B and Type C turbines. Furthermore, these large velocities have two effects on adiabatic efficiencies. One is large reduction in adiabatic efficiency on total-to-static basis compared to that on total-to-total basis. In the present research, dynamic temperatures corresponding to the exit velocities are as much as 6% for Type A and 11% for both Type B and C of adiabatic heat drop (approximately 74 K). The other is loss generation due to large separation at the inlet of the exducer.

By taking these two effects into consideration, reducing the rotor exit velocity and modifying the shape of the exducer in the meridian plane are thought to increase adiabatic efficiencies of 2D turbines by a considerable amount.

## CONCLUSIONS

In this research, toward realization of ultra-micro-scale turbines, three types of 2D small-scale radial turbines are designed, fabricated and experimented. As the result, conclusions described below are obtained.

- Measured adiabatic efficiencies of the fabricated 2D radial turbines are around 15% lower than those of the 3D turbines.
- From CFD analysis, about half of the overall loss occurs at the exducer, and around 40% of the loss at the nozzle trailing edge and the suction side of the blade.
- In 2D turbines, rotor exit absolute velocities inevitably become large, which leads to substantial decrease of total-to-static efficiency. Therefore, in order to improve their efficiencies, reduction in rotor exit velocity and modification of shapes in the meridian plane are required.

## REFERENCES


Epstein, A., et al., "Micro-Heat Engines, Gas Turbines, and Rocket Engines, -The MIT Microengine Project-," *AIAA Paper* 97-1773, 1997.

Epstein, A., et al., "Shirt-button-sized Gas Turbines: The Engineering Challenges of Micro High Speed Rotating Machinery," *Proceedings of the 8th International Symposium on Transport Phenomena and Dynamics of Rotating Machinery (ISROMAC-8)*, 2000.

Ikeda, H., 2003, "Development of Ultra-micro Radial Turbine (in Japanese)," Master Thesis, The University of Tokyo.

Isomura, K., et al., 2001, "Feasibility Study of a Gas Turbine at Micro Scale, " *ASME Paper 2001-GT-101*.

Matsuo, E., 1998, "Characteristics of radial turbines and its' application to aerodynamic designs (in Japanese)," Ph. D. Thesis, The University of Tokyo.

Mizumachi, H., 1958, "Researches on radial gas turbines (in Japanese)," *Report of Institute of Industrial Science, The University of Tokyo*, Vol. 8, No. 1.

Tanaka, S., et al., 2002, "Design and Fabrication Challenges for Micromachined Gas Turbine Generators," *Proceedings of 9th International Symposium on Transport Phenomena and Dynamics of Rotating Machinery (ISROMAC-9).*

Yoshiki, H., et al., 2001, "Toward Ultra-microminiaturization of gas turbines (in Japanese)", *Journal of the Gas Turbine Society of Japan*, 29-4, pp. 228-265.


## ACKNOWLEDGEMENT


This research was supported by New Energy and Industrial Technology Development Organization (NEDO).

The authors wish to thank technical staff Nobuyuki Takama, Tsuneo Suzuki; former undergraduate student of Kogakuin University, Takashi Makino; Master course student of The University of Tokyo, Yosuke Yamamoto; Undergraduate student of Kogakuin University, Satoshi Suzuki for assistance in manufacturing experimental apparatuses and performing experiments, and lecturer at The Department of Aeronautics and Astronautics in The University of Tokyo, Susumu Teramoto for helping CFD calculations.